

---

# CONTEXTUAL MOLECULE REPRESENTATION LEARNING FROM CHEMICAL REACTION KNOWLEDGE

---

Han Tang<sup>\*1,2</sup>, Shikun Feng<sup>\*1</sup>, Bicheng Lin<sup>3</sup>, Yuyan Ni<sup>1,4</sup>, Jingjing Liu<sup>1</sup>, Wei-Ying Ma<sup>1</sup>, and Yanyan Lan<sup>1</sup>

<sup>1</sup>Institute for AI Industry Research (AIR), Tsinghua University, Beijing, China

<sup>2</sup>Department of Computer Science, University of Copenhagen, Copenhagen, Denmark

<sup>3</sup>Department of Computer Science and Technology, Tsinghua University, Beijing, China

<sup>4</sup>Academy of Mathematics and Systems Science, Chinese Academy of Sciences, Beijing, China

## ABSTRACT

In recent years, self-supervised learning has emerged as a powerful tool to harness abundant unlabelled data for representation learning and has been broadly adopted in diverse areas. However, when applied to molecular representation learning (MRL), prevailing techniques such as masked sub-unit reconstruction often fall short, due to the high degree of freedom in the possible combinations of atoms within molecules, which brings insurmountable complexity to the masking-reconstruction paradigm. To tackle this challenge, we introduce *REMO*, a self-supervised learning framework that takes advantage of well-defined atom-combination rules in common chemistry. Specifically, *REMO* pre-trains graph/Transformer encoders on 1.7 million known chemical reactions in the literature. We propose two pre-training objectives: Masked Reaction Centre Reconstruction (MRCR) and Reaction Centre Identification (RCI). *REMO* offers a novel solution to MRL by exploiting the underlying shared patterns in chemical reactions as *context* for pre-training, which effectively infers meaningful representations of common chemistry knowledge. Such contextual representations can then be utilized to support diverse downstream molecular tasks with minimum finetuning, such as affinity prediction and drug-drug interaction prediction. Extensive experimental results on MoleculeACE, ACNet, drug-drug interaction (DDI), and reaction type classification show that across all tested downstream tasks, *REMO* outperforms the standard baseline of single-molecule masked modeling used in current MRL. Remarkably, *REMO* is the pioneering deep learning model surpassing fingerprint-based methods in activity cliff benchmarks.

**Keywords** Self-supervised Pre-training · Chemical Reaction · Molecular Representation Learning

## 1 Introduction

Recently, there has been a surging interest in self-supervised molecule representation learning (MRL) [Rong et al., 2020, Guo et al., 2021, Xu et al., 2021, Lin et al., 2022], with aims at a pre-trained model learned from a large quantity of unlabelled data to support different molecular tasks, such as drug-drug interaction [Ryu et al., 2018], molecule generation [Irwin et al., 2020], and molecular property prediction [Wu et al., 2018]. Though demonstrating promising results, these pre-training methods still exhibit critical drawbacks. For example, as illustrated in Figure 1b, two molecules that have significantly different chemical properties can exhibit very similar structures. This is called *activity cliff* [Stumpfe et al., 2019], a crucial differentiation task in drug discovery, where most neural networks (especially pre-trained models) struggle with poor performance not even comparable to a simple SVM method based on traditional fingerprint features [van Tilborg et al., 2022, Zhang et al., 2023].

Despite different architectures (transformer or graph neural networks), most current methods use a BERT-like masked reconstruction loss for training. This omits the high complexity of atom combinations within molecules in nature which is quite unique compared to a simple sentence comprised of a few words. To better capture the hidden intrinsic

---

\*These authors contributed equally to this work

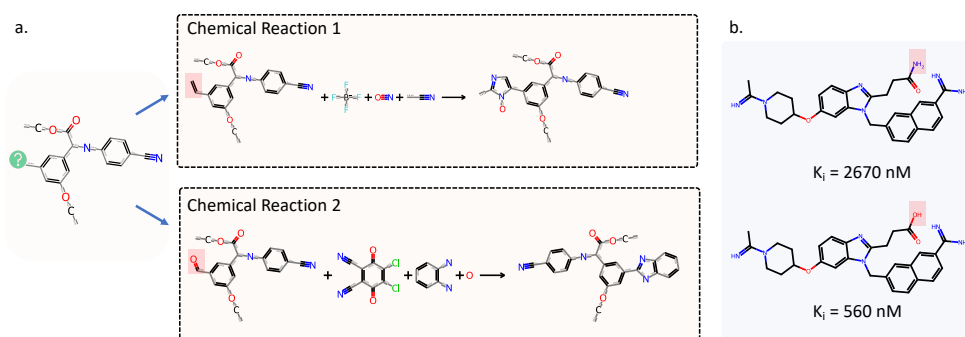


Figure 1: **a**: Adding either carbon or oxygen to the left molecule can lead to the formation of a valid molecule. However, these resulting molecules exhibit distinct reactions and consequently possess varying properties. **b**: Example of an activity cliff pair on the target Thrombin(F2), where  $K_i$  is to measure the equilibrium binding affinity for a ligand that reduces the activity of its binding partner.

characteristics of molecule data, we need to look beneath the surface and understand how molecules are constructed biologically.

For example, unlike the assumption in distributed semantic representation [Firth, 1957] that the meaning of a word is mainly determined by its context, in molecule graphs the combination of adjacent sub-units can be more random [Vollhardt and Schore, 2018]. Another main difference is that while changing one word in a long sentence might have a relatively low impact on the semantic meaning of the full sentence, in molecular structure one minor change might lead to a totally different chemical property. As illustrated in Figure 1a, given a pair of molecules with similar constituents, adding either a carbon or an oxygen atom are both reasonable choices in reconstructing it into a real molecule, but each resulting molecule exhibits very different chemical properties. In such cases, traditional masked reconstruction loss is far from being sufficient as a learning objective.

Is there an essential natural principle that guides the atomic composition within molecules? In fact, most biochemical or physiological properties of a molecule are determined and demonstrated by its reaction relations to other substances (e.g., other small molecules, protein targets, bio-issues) [Vollhardt and Schore, 2018]. Further, these natural relations between different reactants (e.g., molecules) are reflected by chemical reaction equations that are public knowledge in the literature. These chemical reaction relations offer a reliable context for the underlying makeup of molecule sub-structures, especially for reactive centres. As in Figure 1a, the choice of carbon or oxygen can be easily determined by different reactants, even though the two molecules have very similar structures.

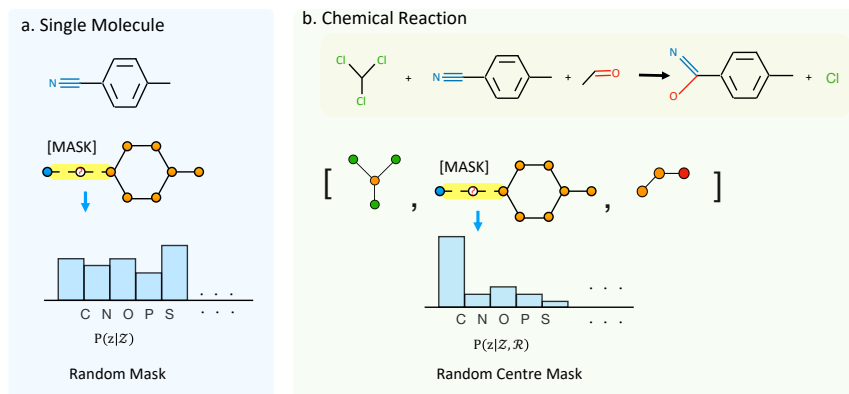


Figure 2: **a**: Traditional masked language model on a single model with objective  $P(z|\mathcal{Z})$ , where  $z$  is the masked substructure and  $\mathcal{Z}$  stands for the remaining ones. **b**: Our proposed Masked Reaction Centre Reconstruction with objective  $P(z|\mathcal{Z}, \mathcal{R})$ , where  $\mathcal{R}$  denotes other reactants in chemical reactions.

Motivated by these insights, we propose a new self-supervised learning method, *REMO*, by harnessing chemical reaction knowledge to model molecular representations. Specifically, given a chemical reaction equation known in the literature, we mask the reaction centres and train the model to reconstruct the missing centres based on the given reactants as context. The key difference between *REMO* and existing methods that apply masked language model to a single molecule is the usage of *sub-molecule interaction context*, as illustrated in Fig 2. By relying on chemical reactants as context, the degree of freedom in possible combinations of atoms within a molecule is significantly reduced, and meaningful sub-structure semantics capturing intrinsic characteristics can be learned in the reconstruction process.

Extensive experiments demonstrate that *REMO* achieves new state-of-the-art results against other pre-training methods on a wide range of molecular tasks, such as activity-cliff, drug-drug interaction, and reaction type classification. And to the best of our knowledge, *REMO* is the first deep learning model to outperform traditional methods on activity-cliff benchmarks such as MoleculeACE and ACNet.

## 2 Related Work

### 2.1 Self-Supervised Learning for Molecule Representation

Since this work is related to masked language model (MLM) [Devlin et al., 2019, Conneau and Lample, 2019], we review recent MLM-based molecular representation learning methods. MLM is a highly effective proxy task, which has recently been applied to molecular pre-training on SMILES sequences, 2D graphs, and 3D conformations.

For pre-training on SMILES sequences, existing work including ChemBERTa [Chithrananda et al., 2020], MG-BERT [Zhang et al., 2021] and Molformer [Ross et al., 2022] directly apply MLM to SMILES sequence data, and conduct similar reconstruction optimization to obtain molecular representations. When applied to 2D graphs, different masked strategies have been proposed. For example, AttrMask [Hu et al., 2020] randomly masks some atoms of the input graph and trains a Graph Neural Network (GNN) model to predict the masked atom types. GROVER [Rong et al., 2020] trains the model to recover masked sub-graph, which consists of k-hop neighboring nodes and edges of the target node. Mole-BERT [Xia et al., 2023] uses a VQ-VAE tokenizer to encode masked atoms with contextual information, thereby increasing vocabulary size and alleviating the unbalanced problem in mask prediction. By capturing topological information in a graph, these methods have the ability to outperform the aforementioned SMILES-based methods.

Recently studies also apply MLM to 3D conformations. For example, Uni-MOL [Zhou et al., 2023] predicts the masked atom in a noisy conformation, while ChemRL-GEM [Fang et al., 2022] predicts the atom distance and bond angles from masked conformation. Yet these methods suffer from limited 3D conformation data.

In summary, MLM has been widely used in molecule representation over different data forms (1D, 2D, 3D). Given a single molecule, some sub-structures are masked, and a reconstruction loss is computed to recover the semantic relations between masked sub-structures and remaining contexts. However, this training objective does not fit the essence of molecule data and may lead to poor performance. For example, MoleculeACE [van Tilborg et al., 2022] and ACNet [Zhang et al., 2023] demonstrate that existing pre-trained models are incomparable to SVM based on fingerprint on activity cliff.

### 2.2 Chemical Reaction Models

Most existing work on modelling chemical reactions is based on supervised learning [Jin et al., 2017, Coley et al., 2019]. For example, Jin et al. [2017] and Coley et al. [2019] use a multiple-step strategy to predict products given reactants and achieve human-expert comparable accuracy without using reaction templates.

Recently, self-supervised learning methods have been proposed to utilize chemical reaction data for pre-training, including Wen et al. [2022], Wang et al. [2022] and Broberg et al. [2022]. Wen et al. [2022] conducts a contrastive pre-training on unlabelled reaction data to improve the results of chemical reaction classification. Wang et al. [2022] focuses on introducing reaction constraints on GNN-based molecular representations, to preserve the equivalence of molecules in the embedding space. Broberg et al. [2022] pre-trains a transformer with a sequence-to-sequence architecture on chemical reaction data, to improve the performance of molecular property prediction.

Although these methods use chemical reaction data for pre-training, *REMO* is different as the objective is to focus on the reaction centre, i.e. masked reaction centre construction, and identification, which better fits chemical reaction data. *REMO* also provides a general framework that can be used in different architectures, such as Transformer and GNNs, to support diverse downstream tasks.

### 3 REMO: Contextual Molecular Modeling

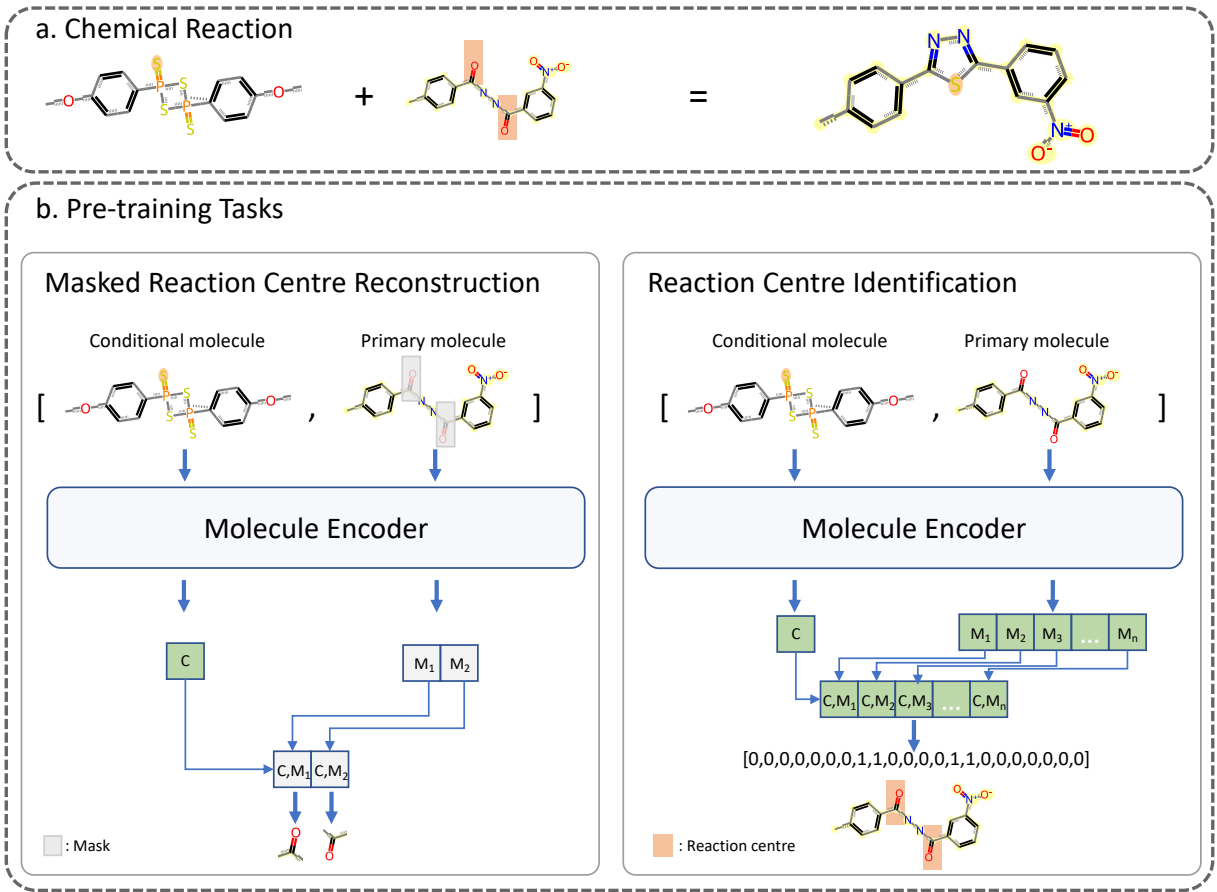


Figure 3: Architecture of *REMO*. **a**: An example chemical reaction consisting of two reactants and one product, where the primary reactant has two reaction centres (marked in red). **b**: Illustrations of two pre-training tasks in *REMO*, *i.e.*, Masked Reaction Centre Reconstruction and Reaction Centre Identification, where , refer to feature concatenation

This section describes the molecule encoder and the pre-training process of *REMO*, specifically, its two pre-training tasks: Masked Reaction Centre Reconstruction (*MRCR*) and Reaction Centre Identification (*RCI*).

#### 3.1 Molecule Encoder

We design *REMO* as a self-supervised learning framework, which is agnostic to the choice of encoder architecture. In this work, we represent each molecule as a 2D graph  $G = (V, E)$ , where  $V$  is the set of atoms and  $E$  is the set of bonds, and each bond or node is represented as a *one-hot initialized embedding* based on its type. Particularly, we experiment with two model architectures for pre-training: one is GNN-based, with Graph Isomorphism Network (GIN) [Xu et al., 2018] as representative; the other is transformer-based, with Graphormer as the backbone [Ying et al., 2021].

GIN [Xu et al., 2018] learns representations for each node and the whole graph through a neighbor aggregation strategy. Specifically, each node  $v \in V$  updates its representation based on its neighbors and itself in the aggregation step, and the  $l$ -th layer of a GIN is defined as:

$$h_v^{(l)} = \text{MLP}^{(l)} \left( (1 + \epsilon^{(l)}) \cdot h_v^{(l-1)} + \sum_{u \in \mathcal{N}(v)} h_u^{(l-1)} + \sum_{u \in \mathcal{N}(v)} e_{uv} \right) \quad (1)$$

where  $h_v^{(l)}$  is the representation of node  $v$  in the  $l$ -th layer,  $e_{uv}$  is the representation of the edge between  $u$  and  $v$ , and  $\mathcal{N}(v)$  stands for the neighbors of  $v$ .

Then, we obtain the graph-level representation through a "READOUT" function, with the average of node features used as the pooling layer:

$$h_G = \text{READOUT} \left( \left\{ h_v^{(K)} \mid v \in G \right\} \right) \quad (2)$$

Graphormer [Ying et al., 2021] is the first deep learning model built upon a standard Transformer that greatly outperforms all conventional GNNs on graph-level prediction tasks, and has won first place in the KDD Cup-OGB-LSC quantum chemistry track [Hu et al., 2021]. The basic idea is to encode graph structural information to positional embeddings, to facilitate Transformer architecture. Specifically, Graphormer introduces three types of positional embeddings, and we simply follow the original architecture. The attention in Graphormer is calculated by:

$$A_{ij} = \frac{(h_i W_Q)(h_j W_K)^T}{\sqrt{d}} + b_{\phi(v_i, v_j)} + c_{ij}, \quad c_{ij} = \frac{1}{N} \sum_{n=1}^N x_{e_n} (w_n^E)^T \quad (3)$$

where  $h_i$  and  $h_j$  are centrality embeddings to capture the node importance in the graph,  $b_{\phi(v_i, v_j)}$  is spatial encoding calculated by the shortest path (SP) to capture the structural relation between nodes, and  $c_{ij}$  is the edge embedding.  $x_{e_n}$  is the feature of the  $n$ -th edge  $e_n$  in  $\text{SP}_{ij}$ ,  $w_n^E \in \mathbb{R}^{d_E}$  is the  $n$ -th weight embedding, and  $d_E$  is the dimensionality of edge feature. Apart from adjustments on the attention mechanism, Graphormer follows the original Transformer [Vaswani et al., 2017] to obtain embeddings.

### 3.2 Learning Objective

Our design philosophy of the learning objective is as follows: reaction centres are the core of a chemical reaction, which depict meaningful structural and activity-related relations within a molecule. Specifically, chemical reaction describes a process in which one or more substances (*i.e.*, reactants) are transformed to one or more different substances (*i.e.*, products). This process involves exchanging electrons between or within molecules, and breaking old chemical bonds while forming new ones. It has been observed that only parts of molecules are directly involved in reactions (known as ‘reaction centres’) in organic chemistry. Therefore, reaction centres are the key to revealing the behaviors of molecule reactivity properties during the chemical reaction process.

Formally, each chemical reaction is viewed as two graphs: reactant graph  $G_r$  and product graph  $G_p$ , which are unconnected when there are multiple reactants or products. Since reaction centres are usually not provided by chemical reaction data, we utilize a widely used technique [Jin et al., 2017, Shi et al., 2020] to detect corresponding reaction centres. Specifically, the reaction centre for a chemical reaction process is represented as a set of atom pairs  $(a_i, a_j)$ , where the bond type between  $a_i$  and  $a_j$  differs between the aligned reactant graph  $G_r$  and the product graph  $G_p$ . Intrinsically, the reaction centre is the minimum set of graph edits to transform reactants to products.

### 3.3 Masked Reaction Centre Reconstruction

We propose a new pre-training task, where each reactant in a chemical reaction is treated as the primary molecule, and the remaining reactants are treated as its contexts or conditional molecules. The reaction centre atoms in the primary molecule and their adjacent bonds are masked with a special token, denoted as  $[MASK]$ . Then all the conditional molecules are fed into the molecule encoder to obtain a global representation. Specifically for GIN encoder, the node vector of each atom in conditional molecules are pooled to produce a global representation  $c$ . While for Graphormer, the process is a bit different. To adapt to the transformer architecture, we introduce a virtual node to connect all the atoms together, and the representation of the virtual node in the last layer is treated as the global representation.

The masked primary molecule with  $k$  reaction centres is directly fed into the molecule encoder (GIN or Graphormer), and the final hidden vectors corresponding to each  $[MASK]$  token are produced by concatenating the vectors of atoms belonging to this reaction centre, denoted as  $M_j, \forall j = 1, \dots, k$ .

After that, both  $c$  and each  $M_j, j = 1, \dots, k$  are fed into a 2-layer MLP to output a softmax over the vocabulary to predict the probability of the masked reaction centre. Specifically, the vocabulary is produced by enumerating all the topological combinations of the atoms and their adjacent bonds. The model is expected to predict the exact atom type and the adjacent bonds during the pre-training stage:

$$P(g_j) = \text{softmax}(MLP(c, M_j)), \forall j = 1, \dots, k, \quad (4)$$

where  $g_j$  stands for the graph representation of the  $j$ -th reaction centre, including both atom types and adjacent bonds. Finally, the sum of negative likelihood loss is used for training.

### 3.4 Reaction Centre Identification

Another novel pre-training objective in *REMO* directly conducts classification on each atom without introducing any  $[MASK]$  label. For each primary molecule in a chemical reaction, all the conditional molecules are fed into

the molecule encoder to obtain a global representation  $c$ , similar to that in Masked Reaction Centre Reconstruction. The primary molecule is directly fed into the molecule encoder (GIN or Graphormer), and the final hidden vectors corresponding to each atom are produced, denoted as  $R_j, \forall j = 1, \dots, N$ , where  $N$  stands for the number of atoms in the primary molecule.

After that, both  $c$  and each  $R_j, j = 1, \dots, N$  are fed into a 2-layer MLP to predict whether an atom belongs to a reaction centre, as follows:

$$P(y_j) = \text{softmax}(MLP(c, R_j)), \forall j = 1, \dots, N, \quad (5)$$

where  $y_j = 1/0$  denotes whether the  $j$ -th atom is a reaction centre. During training, the sum of the negative likelihood loss is utilized as the objective function.

## 4 Experiments

We evaluate *REMO* against state-of-the-art (SOTA) baselines on multiple molecular tasks, including activity cliff prediction, drug-drug interaction, and reaction type classification. Extensive experiments show that *REMO* achieves new SOTA on all tasks.

### 4.1 Implementation

Firstly, we introduce the pre-training of *REMO*. We utilize USPTO [Lowe, 2017] as our pre-training data, which is a subset and pre-processed version of chemical reactions from US patents (1976 - Sep. 2016). From different versions of USPTO, we select the largest one, *i.e.*, USPTO-full, which contains 1.9 million chemical reactions. After removing the reactions that fail to locate reaction centres, there remain 1,721,648 reactions in total, which constitutes our pre-training dataset, which covers 0.7 million distinct molecules as reactants.

We implement three versions of *REMO*, denoted as *REMO*<sub>M</sub>, *REMO*<sub>I</sub> and *REMO*<sub>IM</sub>, to represent different training objectives (*i.e.*, masked reaction centre reconstruction, reaction centre identification, and both). As for molecule encoders, we implement both GIN and Graphormer, adopting the configuration from the original papers. Specially for Graphormer, we choose the *small* configuration. We apply Adam optimizer throughout pre-training and fine-tuning. The learning rate is set to 3e-4, and the batch size is set to 128. We randomly split 10,000 reactions as the validation set, and pre-training lasts for 5 epochs.

### 4.2 Activity Cliff Prediction

Activity cliff is a known challenging task, because all given molecule pairs are structurally similar but exhibiting significantly different activities. An accurate activity cliff predictor should be sensitive to the structure-activity landscape. SOTA deep-learning-based molecular representation learning methods have failed to yield better results than fingerprint-based methods on this task [van Tilborg et al., 2022, Zhang et al., 2023]. In our experiments, we use two benchmarks, MoleculeACE and ACNet.

#### 4.2.1 Evaluation on MoleculeACE

**Data** MoleculeACE [van Tilborg et al., 2022] includes 30 tasks, each of which provides binding affinities of different molecules to a specific protein target. Among these molecules, there are some activity-cliff pairs, spreading to the training set and test set. The size of every single benchmark ranges from 615 to 3,658, and the range of cliff ratio (the percentage of activity cliff molecules to all molecules) is from 9% to 52%. In experiments, we follow the train-test split of the default setting of MoleculeACE, and accordingly stratified split the training set into train and validation sets by ratio 4:1.

**Baselines** We compare with the baselines tested by MoleculeACE [van Tilborg et al., 2022], including fingerprint-based methods, SMILES-based methods and graph-based methods. We also include GIN [Xu et al., 2018] and D-MPNN [Yang et al., 2019] as stronger baselines. Since we also use Graphormer [Ying et al., 2021] as our molecule encoder, we implement its supervised version for comparison. In addition, to prove the performance gain is not from changing the pre-training dataset, we pre-train the same backbones GIN and Graphormer adopting the molecules from the USPTO-full dataset, though using an alternative pre-training method by Hu et al. [2020], these two baselines are denoted as AttrMask-GIN and AttrMask-Graphormer in the table.

**Finetuning** The pre-trained model of *REMO* is followed by a 2-layer MLP to obtain the logits. Since binding-affinity prediction is a regression task, we use RMSE as the loss for finetuning. For evaluation, we follow the default setting

		RMSE ↓	RMSE <sub>cliff</sub> ↓
Fingerprint based	ECFP+MLP	0.772	0.831
	ECFP+SVM	<u>0.675</u>	<u>0.762</u>
SMILES based	SMILES+Transformer	0.868	0.953
	SMILES+CNN	0.937	0.962
	SMILES+LSTM	0.744	0.881
Graph based	GAT	1.050	1.060
	GCN	1.010	1.042
	AFP	0.970	1.000
	MPNN	0.960	0.998
	GIN	0.815	0.901
	Graphormer	0.805	0.848
	D-MPNN	0.750	0.829
Pre-training based	AttrMask-GIN	0.820	0.930
	AttrMask-Graphormer	0.695	0.821
Ours	REMO <sub>M</sub> -GIN	0.807	0.922
	REMO <sub>I</sub> -GIN	0.767	0.878
	REMO <sub>M</sub> -Graphormer	0.679	0.764
	REMO <sub>I</sub> -Graphormer	<u>0.675</u>	0.768
	REMO <sub>IM</sub> -Graphormer	<b>0.647</b>	<b>0.747</b>

Table 1: Comparison between *REMO* and baselines on MoleculeACE. The best and second-best results are indicated in bold and underlined, respectively.

Models	AUC ↑
GROVER [Rong et al., 2020]	0.753(0.010)
ChemBERT [Guo et al., 2021]	0.656(0.029)
MAT [Maziarka et al., 2020]	0.730(0.069)
Pretrain8 [Zhang et al., 2022]	0.782(0.031)
pretrainGNNs [Hu et al., 2020]	0.758(0.015)
S.T. [Honda et al., 2019]	0.822(0.022)
GraphLoG [Xu et al., 2021]	<u>0.752(0.040)</u>
GraphMVP [Liu et al., 2021]	0.724(0.026)
ECFP	0.813(0.024)
REMO <sub>IM</sub> -Graphormer	<b>0.828(0.020)</b>

Table 2: Comparison between *REMO* and baselines on the *Few* subset of ACNet, with AUC-ROC(%) as the evaluation metric.

of MoleculeACE and report two metrics: averaged RMSE over the entire test set and averaged RMSE of the cliff molecules subset, denoted as RMSE<sub>cliff</sub>.

**Results** Table 1 shows that: (1) Our contextual pretraining strategy is much more suitable for activity cliff, as compared to traditional masked strategy on single molecules. For example, the AttrMask model, a pre-trained GIN (0.820/0.930), performs worse than the original GIN (0.815/0.901). Whereas if we pre-train GIN within *REMO*, better results (0.767/0.878) are achieved, as shown in *REMO<sub>I</sub>*. (2) None of the deep learning baselines is comparable to the fingerprint-based method ECFP+SVM (0.675/0.762) except for *REMO*, both *REMO<sub>I</sub>*-Graphormer (0.675/0.768) and *REMO<sub>M</sub>*-Graphormer (0.679/0.764) show comparable results to ECFP+SVM, and *REMO<sub>IM</sub>*-Graphormer (0.647/0.747) achieves the SOTA result, as the best as we know of.

#### 4.2.2 Evaluation on ACNet

**Data** ACNet [Zhang et al., 2023] serves as another benchmark for activity cliff evaluation. Different from MoleculeACE, ACNet specifically focuses on classification task of determining whether a given molecular pair qualifies as an activity cliff pair. In our experiment, we employ a subset of tasks known as *Few* for evaluation, which is comprised of 13 distinct tasks with a total of 835 samples. Due to the limited size of training data, learning a model from scratch is challenging. Therefore, it is especially suitable to evaluate the transfer learning capability of pre-trained models. We adhere to the split method in ACNet, dividing each task into separate train, validation, and test sets.

Method	Accuracy $\uparrow$	Precision $\uparrow$	Recall $\uparrow$	F1-Score $\uparrow$
Graphormer	0.846	0.725	0.680	0.684
DeepDDI	0.877	0.799	0.759	0.766
DeepWalk	0.800	0.822	0.710	0.747
LINE	0.751	0.687	0.545	0.580
MUFFIN	0.939	0.926	0.908	0.911
GraphLoG	0.908	0.879	0.846	0.846
Mol-BERT	0.922	0.885	0.861	0.863
<i>REMO</i> <sub>IM</sub> -Graphormer	<b>0.953</b>	<b>0.932</b>	<b>0.932</b>	<b>0.928</b>

Table 3: Evaluation of *REMO* on Drug-Drug Interaction task.

**Baselines** We use the same baselines as the original ACNet, including self-supervised pre-trained methods such as Grover [Rong et al., 2020], ChemBERT [Guo et al., 2021], MAT [Maziarka et al., 2020], Pretrain8 [Zhang et al., 2022], PretrainGNNs [Hu et al., 2020], S.T. [Honda et al., 2019], GraphLoG [Xu et al., 2021], and GraphMVP [Liu et al., 2021]. Additionally, we include another baseline method that utilizes ECFP fingerprint-based MLP for training. All the results here are from the original ACNet paper.

**Finetuning** Following the practice of ACNet, we extract the embedding of each molecule in the input pair with pre-trained *REMO*. Since Graphormer demonstrates superior performance to GIN, we only evaluate *REMO*<sub>IM</sub> with Graphormer as the molecule encoder hereafter. We concatenate these embeddings and feed them into a 2-layer MLP model to predict whether the pair exhibits an activity cliff. Each experiment is repeated three times, and the mean and deviation values are reported. Prediction accuracy is measured by ROC-AUC(%). We run finetuning with 3 random seeds, and take the average along with the standard deviation (reported in bracket).

**Results** Table 2 shows that *REMO* clearly outperforms all other pre-trained methods, yielding the best results. This further demonstrates *REMO*’s proficiency in capturing the Quantitative Structure-Activity Relationship (QSAR).

### 4.3 Drug-Drug Interaction

**Data** We collect the multi-class drug-drug interaction (DDI) data following the work of MUFFIN [Chen et al., 2021]. The dataset, which contains 172,426 DDI pairs with 81 relation types, is filtered from DrugBank [Wishart et al., 2018] that relationships of less than 10 samples are eliminated. We randomly split the dataset into training, validation, and test set by 6:2:2.

**Baselines** To examine the effectiveness of our model, we compare *REMO*<sub>IM</sub>-Graphormer with several baselines, including well-known graph based methods DeepWalk [Perozzi et al., 2014], LINE [Tang et al., 2015] and MUFFIN, and a typical deep learning based method DeepDDI [Ryu et al., 2018].

**Finetuning** We concatenate the paired global embedding of each molecule and feed it into a 2-layer MLP. Then a cross-entropy loss is utilized for fine-tuning. Typical classification metrics such as Precision, Recall, F1, and Accuracy are used for evaluation.

**Results** As shown in Table 3, our pre-trained model outperforms all the baselines, indicating that *REMO* effectively captures molecule interaction information from chemical reaction data.

### 4.4 Reaction Type Classification

**Data** The goal of reaction type classification is to predict the class of a given chemical reaction from the set of reactants and products. We evaluate our model on USPTO-1k-TPL, a dataset contains 400,604 reactions in the training set and 44,511 reactions in the testing set, and the number of classes is 1000.

**Baselines** We apply the setting of *REMO*<sub>IM</sub>-Graphormer to this benchmark, and compare it with some methods that are specially designed to learn reaction fingerprints, which are RXNFP [Schwaller et al., 2021], AP3-256 [Schneider et al., 2015], and DRFP [Probst et al., 2021], and MolR-TAG [Wang et al., 2022], another model pre-trained on the chemical reaction dataset as the same as we do.

**Finetuning** We follow the approach by Wang et al. [2022] for finetuning. We use *REMO*<sub>IM</sub>-Graphormer as the pre-trained model, and assign two virtual nodes to connect with all atoms in reactants, and products each. Then we concatenate the representations of the two virtual nodes and pass it to an MLP with two 1,024-unit hidden layers.

Method	Accuracy $\uparrow$
RXNFP [Schwaller et al., 2021]	0.989
AP3-256-MLP [Schneider et al., 2015]	0.809
DRFP-MLP [Probst et al., 2021]	0.977
MolR-TAG [Wang et al., 2022]	0.962
<i>REMO</i> <sub>IM</sub> -Graphormer	0.980

Table 4: Results of Reaction Type Classification, Result of baselines is taken from Wang et al. [2022]. We take the results of the best performance models from each paper.

**Results** The results in accuracy are reported in Table 4. Notably, *REMO*<sub>IM</sub>-Graphormer surpasses most baselines such as AP3-256 and DRFP, and is close to RXNFP, even if they are specifically designed to learn reaction fingerprints. Moreover, our method bypasses another baseline pre-trained model from the same USPTO dataset, MolR, which proves the superiority in performance for *REMO*<sub>IM</sub>-Graphormer. The results show our method can achieve on par performance with state-of-the-art reaction fingerprint learning methods.

#### 4.5 Ablation Studies

In order to further explain the advantage of *REMO* compared to the traditional masked language model on single molecule, we conduct an ablation study to compare AttrMask and *REMO*, where Graphormer is utilized as backbones of both methods to ensure a fair comparison.

Firstly, we show the comparison results on MoleculeACE. We pre-trained a model with the same graphormer architecture as *REMO*<sub>M</sub>-Graphormer, but reconstructing the masked reaction centres without conditional molecules. This model is denoted as Graphormer-p, to compare with *REMO*<sub>M</sub>-Graphormer. The only difference between Graphormer-p and *REMO*<sub>M</sub>-Graphormer is the involvement of conditional molecules during pre-training. The model without pre-train is denoted as Graphormer-s.

As shown in Table 5, even though pre-trained Graphormer (i.e. Graphormer-p) outperforms supervised Graphormer (i.e. Graphormer-s), it is inferior to *REMO*<sub>M</sub>-Graphormer, demonstrating the superiority of our contextual pre-training objective.

As discussed in "Introduction" that traditional masking methods provide insufficient information to reconstruct the masked substructures, while our pre-training method further involves other reactants in the chemical reaction that centres on the masked atoms to determine the masked substructure, providing more contextual information to determine the masked tokens. To explicitly demonstrate the superiority, we propose to compare the information entropy of the probability of the masked sub-structure. In contrast with the traditional masking whose target probability is  $Q = P(z|\mathcal{Z})$ , our method models a conditional probability  $P = P(z|\mathcal{Z}, \mathcal{R})$ , where  $z$  is the masked token,  $\mathcal{Z}$  stands for the remaining substructures in the molecule and  $\mathcal{R}$  stands for other reactants in the chemical reactions. Then the information entropy in our case is lower than that in the traditional case, i.e.  $H(P) \leq H(Q)$ , meaning that the choice of masked sub-units becomes more definite under the context of chemical reactions. This allows the model to learn explicit chemical semantics of molecular sub-structures. More detailed discussion is proved in appendix A.

To qualitatively evaluate their difference, we select 10,000 reactions from USPTO-full and conduct the reconstructions separately. The results in Figure 4 show clear distribution shifts to the left with the average information entropy dropping from 2.03 to 1.29, indicating that introducing reaction information contributes to the reaction centre reconstruction.

	RMSE $\downarrow$	RMSE <sub>cliff</sub> $\downarrow$
Graphormer-s	0.805(0.017)	0.848(0.003)
Graphormer-p	0.695(0.004)	0.821(0.004)
<i>REMO</i> <sub>M</sub> -Graphormer	0.679(0.006)	0.764(0.004)

Table 5: Ablation study of *REMO* on MoleculeACE.

## 5 Conclusion

We propose *REMO*, a novel self-supervised molecular representation learning method (MRL) that leverages the unique characteristics of chemical reactions as knowledge context for pre-training. By involving chemical reactants as context,

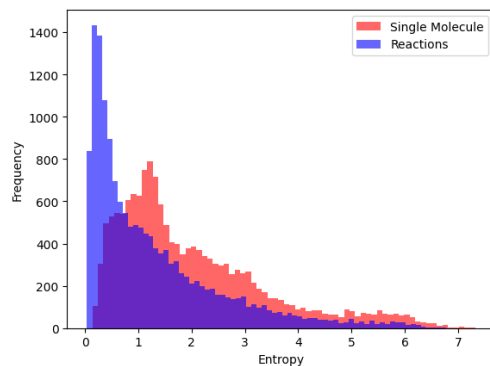


Figure 4: The information entropy of reconstructing reaction centres from reactions

we use both masked reaction centre reconstruction and reaction centre identification objectives for pre-training, which reduces the degree of freedom in possible combinations of atoms in a molecule as in traditional MLM approaches for MRL. Extensive experimental results reveal that *REMO* achieves state-of-the-art performance with less pre-training data on a variety of downstream tasks, including activity cliff prediction, drug-drug interaction, and reaction type classification, demonstrating the superiority of contextual modelling with chemical reactions.

## References

- Johan Broberg, Maria Margareta Bånkestad, and Erik Ylipää Hellqvist. Pre-training transformers for molecular property prediction using reaction prediction. In *ICML 2022 2nd AI for Science Workshop, 2022*. URL <https://openreview.net/forum?id=96HIXODoKOS>.
- Yujie Chen, Tengfei Ma, Xixi Yang, Jianmin Wang, Bosheng Song, and Xiangxiang Zeng. Muffin: multi-scale feature fusion for drug–drug interaction prediction. *Bioinformatics*, 37(17):2651–2658, 2021.
- Seyone Chithrananda, Gabriel Grand, and Bharath Ramsundar. Chemberta: Large-scale self-supervised pretraining for molecular property prediction. *arXiv preprint arXiv:2010.09885*, 2020.
- Connor W. Coley, Wengong Jin, Luke Rogers, Timothy F. Jamison, Tommi S. Jaakkola, William H. Green, Regina Barzilay, and Klavs F. Jensen. A graph-convolutional neural network model for the prediction of chemical reactivity. *Chem. Sci.*, 10:370–377, 2019. doi: 10.1039/C8SC04228D. URL <http://dx.doi.org/10.1039/C8SC04228D>.
- Alexis Conneau and Guillaume Lample. *Cross-lingual language model pretraining*. Curran Associates Inc., Red Hook, NY, USA, 2019.
- Thomas Cover and Joy Thomas. *Entropy, Relative Entropy, and Mutual Information*, volume 2, pages 13–55. 04 2005. ISBN 9780471241959. doi: 10.1002/047174882X.ch2.
- Jacob Devlin, Ming-Wei Chang, Kenton Lee, and Kristina Toutanova. BERT: Pre-training of deep bidirectional transformers for language understanding. In *Proceedings of the 2019 Conference of the North American Chapter of the Association for Computational Linguistics: Human Language Technologies, Volume 1 (Long and Short Papers)*, pages 4171–4186, Minneapolis, Minnesota, June 2019. Association for Computational Linguistics. doi: 10.18653/v1/N19-1423. URL <https://aclanthology.org/N19-1423>.
- Xiaomin Fang, Lihang Liu, Jieqiong Lei, Donglong He, Shanzhuo Zhang, Jingbo Zhou, Fan Wang, Hua Wu, and Haifeng Wang. Geometry-enhanced molecular representation learning for property prediction. *Nature Machine Intelligence*, 4(2):127–134, 2022.
- J. R. Firth. A synopsis of linguistic theory, 1930-1955. 1957.
- Jiang Guo, A Santiago Ibanez-Lopez, Hanyu Gao, Victor Quach, Connor W Coley, Klavs F Jensen, and Regina Barzilay. Correction to automated chemical reaction extraction from scientific literature. *Journal of Chemical Information and Modeling*, 61(8):4124–4124, 2021.
- Shion Honda, Shoi Shi, and Hiroki R Ueda. Smiles transformer: Pre-trained molecular fingerprint for low data drug discovery. *arXiv preprint arXiv:1911.04738*, 2019.
- Zhenyu Hou, Xiao Liu, Yukuo Cen, Yuxiao Dong, Hongxia Yang, Chunjie Wang, and Jie Tang. Graphmae: Self-supervised masked graph autoencoders. In *Proceedings of the 28th ACM SIGKDD Conference on Knowledge Discovery and Data Mining*, pages 594–604, 2022.

- Weihua Hu, Bowen Liu, Joseph Gomes, Marinka Zitnik, Percy Liang, Vijay Pande, and Jure Leskovec. Strategies for pre-training graph neural networks. In *International Conference on Learning Representations*, 2020. URL <https://openreview.net/forum?id=HJLWJ5FDH>.
- Weihua Hu, Matthias Fey, Hongyu Ren, Maho Nakata, Yuxiao Dong, and Jure Leskovec. Ogb-lsc: A large-scale challenge for machine learning on graphs. *arXiv preprint arXiv:2103.09430*, 2021.
- John J Irwin, Khanh G Tang, Jennifer Young, Chinzorig Dandarchuluun, Benjamin R Wong, Munkhzul Khurelbaatar, Yurii S Moroz, John Mayfield, and Roger A Sayle. Zinc20—a free ultralarge-scale chemical database for ligand discovery. *Journal of chemical information and modeling*, 60(12):6065–6073, 2020.
- Wengong Jin, Connor W. Coley, Regina Barzilay, and Tommi Jaakkola. Predicting organic reaction outcomes with weisfeiler-lehman network. In *Proceedings of the 31st International Conference on Neural Information Processing Systems, NIPS'17*, page 2604–2613, Red Hook, NY, USA, 2017. Curran Associates Inc. ISBN 9781510860964.
- Xinyuan Lin, Chi Xu, Zhaoping Xiong, Xinfeng Zhang, Ningxi Ni, Bolin Ni, Jianlong Chang, Ruiqing Pan, Zidong Wang, Fan Yu, et al. Pangu drug model: learn a molecule like a human. *bioRxiv*, pages 2022–03, 2022.
- Shengchao Liu, Hanchen Wang, Weiyang Liu, Joan Lasenby, Hongyu Guo, and Jian Tang. Pre-training molecular graph representation with 3d geometry. *arXiv preprint arXiv:2110.07728*, 2021.
- Daniel Lowe. Chemical reactions from us patents (1976-sep2016). <https://doi.org/10.6084/m9.figshare.5104873.v1>, 2017. Dataset.
- Łukasz Maziarka, Tomasz Danel, Sławomir Mucha, Krzysztof Rataj, Jacek Tabor, and Stanisław Jastrzębski. Molecule attention transformer. *arXiv preprint arXiv:2002.08264*, 2020.
- Bryan Perozzi, Rami Al-Rfou, and Steven Skiena. Deepwalk: Online learning of social representations. In *Proceedings of the 20th ACM SIGKDD international conference on Knowledge discovery and data mining*, pages 701–710, 2014.
- Daniel Probst, Philippe Schwaller, and Jean-Louis Reymond. Reaction classification and yield prediction using the differential reaction fingerprint drfp. 07 2021. doi: 10.33774/chemrxiv-2021-mc870.
- Yu Rong, Yatao Bian, Tingyang Xu, Weiyang Xie, Ying Wei, Wenbing Huang, and Junzhou Huang. Self-supervised graph transformer on large-scale molecular data. *Advances in Neural Information Processing Systems*, 33, 2020.
- Jerret Ross, Brian Belgodere, Vijil Chenthamarakshan, Inkit Padhi, Youssef Mroueh, and Payel Das. Molformer: Large scale chemical language representations capture molecular structure and properties. 2022.
- Jae Yong Ryu, Hyun Uk Kim, and Sang Yup Lee. Deep learning improves prediction of drug–drug and drug–food interactions. *Proceedings of the National Academy of Sciences*, 115(18):E4304–E4311, 2018.
- Nadine Schneider, Daniel M. Lowe, Roger A. Sayle, and Gregory A. Landrum. Development of a novel fingerprint for chemical reactions and its application to large-scale reaction classification and similarity. *Journal of Chemical Information and Modeling*, 55(1):39–53, 2015. doi: 10.1021/ci5006614. URL <https://doi.org/10.1021/ci5006614>.
- Philippe Schwaller, Daniel Probst, Alain C. Vaucher, Vishnu H. Nair, David Kreutter, Teodoro Laino, and Jean-Louis Reymond. Mapping the space of chemical reactions using attention-based neural networks. *Nature Machine Intelligence*, 3(2):144–152, Feb 2021. ISSN 2522-5839. doi: 10.1038/s42256-020-00284-w. URL <https://doi.org/10.1038/s42256-020-00284-w>.
- Chence Shi, Minkai Xu, Hongyu Guo, Ming Zhang, and Jian Tang. A graph to graphs framework for retrosynthesis prediction. In *Proceedings of the 37th International Conference on Machine Learning, ICML'20*. JMLR.org, 2020.
- Dagmar Stumpfe, Huabin Hu, and Jürgen Bajorath. Evolving concept of activity cliffs. *ACS Omega*, 4(11):14360–14368, 2019. ISSN 2470-1343. doi: 10.1021/acsomega.9b02221. URL <https://doi.org/10.1021/acsomega.9b02221>.
- Jian Tang, Meng Qu, Mingzhe Wang, Ming Zhang, Jun Yan, and Qiaozhu Mei. Line: Large-scale information network embedding. In *Proceedings of the 24th international conference on world wide web*, pages 1067–1077, 2015.
- Derek van Tilborg, Alisa Alenicheva, and Francesca Grisoni. Exposing the limitations of molecular machine learning with activity cliffs. *Journal of chemical information and modeling*, 62(23):5938–5951, 2022. doi: 10.1021/acs.jcim.2c01073.
- Ashish Vaswani, Noam Shazeer, Niki Parmar, Jakob Uszkoreit, Llion Jones, Aidan N Gomez, Łukasz Kaiser, and Illia Polosukhin. Attention is all you need. In I. Guyon, U. Von Luxburg, S. Bengio, H. Wallach, R. Fergus, S. Vishwanathan, and R. Garnett, editors, *Advances in Neural Information Processing Systems*, volume 30. Curran Associates, Inc., 2017. URL [https://proceedings.neurips.cc/paper\\_files/paper/2017/file/3f5ee243547dee91fbd053c1c4a845aa-Paper.pdf](https://proceedings.neurips.cc/paper_files/paper/2017/file/3f5ee243547dee91fbd053c1c4a845aa-Paper.pdf).

- K. Peter C. Vollhardt and Neil E. Schore. *Organic Chemistry: Structure and Function*. W. H. Freeman, 8 edition, 2018. ISBN 1319079458.
- Hongwei Wang, Weijiang Li, Xiaomeng Jin, Kyunghyun Cho, Heng Ji, Jiawei Han, and Martin Burke. Chemical-reaction-aware molecule representation learning. In *International Conference on Learning Representations*, 2022. URL <https://openreview.net/forum?id=6sh3pIzKS->.
- Mingjian Wen, Samuel M. Blau, Xiaowei Xie, Shyam Dwaraknath, and Kristin A. Persson. Improving machine learning performance on small chemical reaction data with unsupervised contrastive pretraining. *Chem. Sci.*, 13:1446–1458, 2022. doi: 10.1039/D1SC06515G. URL <http://dx.doi.org/10.1039/D1SC06515G>.
- David S Wishart, Yannick D Feunang, An C Guo, Elvis J Lo, Ana Marcu, Jason R Grant, Tanvir Sajed, Daniel Johnson, Carin Li, Zinat Sayeeda, et al. Drugbank 5.0: a major update to the drugbank database for 2018. *Nucleic acids research*, 46(D1):D1074–D1082, 2018.
- Zhenqin Wu, Bharath Ramsundar, Evan N Feinberg, Joseph Gomes, Caleb Geniesse, Aneesh S Pappu, Karl Leswing, and Vijay Pande. Moleculenet: a benchmark for molecular machine learning. *Chemical science*, 9(2):513–530, 2018.
- Jun Xia, Chengshuai Zhao, Bozhen Hu, Zhangyang Gao, Cheng Tan, Yue Liu, Siyuan Li, and Stan Z Li. Mole-bert: Rethinking pre-training graph neural networks for molecules. 2023.
- Keyulu Xu, Weihua Hu, Jure Leskovec, and Stefanie Jegelka. How powerful are graph neural networks? *CoRR*, abs/1810.00826, 2018. URL <http://arxiv.org/abs/1810.00826>.
- Minghao Xu, Hang Wang, Bingbing Ni, Hongyu Guo, and Jian Tang. Self-supervised graph-level representation learning with local and global structure. In *International Conference on Machine Learning*, pages 11548–11558. PMLR, 2021.
- Kevin Yang, Kyle Swanson, Wengong Jin, Connor W. Coley, Philipp Eiden, Hua Gao, Angel Guzman-Perez, Timothy Hopper, Brian P. Kelley, Miriam Mathea, Andrew Palmer, Volker Settels, T. Jaakkola, Klavs F. Jensen, and Regina Barzilay. Analyzing learned molecular representations for property prediction. *Journal of Chemical Information and Modeling*, 59:3370–3388, 2019. URL <https://api.semanticscholar.org/CorpusID:198986021>.
- Chengxuan Ying, Tianle Cai, Shengjie Luo, Shuxin Zheng, Guolin Ke, Di He, Yanming Shen, and Tie-Yan Liu. Do transformers really perform badly for graph representation? In A. Beygelzimer, Y. Dauphin, P. Liang, and J. Wortman Vaughan, editors, *Advances in Neural Information Processing Systems*, 2021. URL <https://openreview.net/forum?id=0eWoo0xFwDa>.
- Xiao-Chen Zhang, Cheng-Kun Wu, Zhi-Jiang Yang, Zhen-Xing Wu, Jia-Cai Yi, Chang-Yu Hsieh, Ting-Jun Hou, and Dong-Sheng Cao. Mg-bert: leveraging unsupervised atomic representation learning for molecular property prediction. *Briefings in bioinformatics*, 22(6):bbab152, 2021.
- Ziqiao Zhang, Yatao Bian, Ailin Xie, Pengju Han, Long-Kai Huang, and Shuigeng Zhou. Can pre-trained models really learn better molecular representations for ai-aided drug discovery? *arXiv preprint arXiv:2209.07423*, 2022.
- Ziqiao Zhang, Bangyi Zhao, Ailin Xie, Yatao Bian, and Shuigeng Zhou. Activity cliff prediction: Dataset and benchmark. *arXiv preprint arXiv:2302.07541*, 2023.
- Gengmo Zhou, Zhifeng Gao, Qiankun Ding, Hang Zheng, Hongteng Xu, Zhewei Wei, Linfeng Zhang, and Guolin Ke. Uni-mol: A universal 3d molecular representation learning framework. 2023.

## A The Superiority of REMO at Pre-training Phase

In molecule graphs, the combination of adjacent sub-units can be relatively random. This poses a challenge to traditional molecular masking methods, as it provides insufficient information to reconstruct the masked atoms. In contrast, our pre-training method further involves other reactants in the chemical reaction that centres on the masked atoms to determine the masked substructure, providing more contextual information to determine the masked tokens.

To explicitly demonstrate the superiority, we formulate the methods as follows. Denote the masked token as  $z$ , the remaining substructures in the molecule as  $\mathcal{Z}$ , and other reactants in the chemical reactions as  $\mathcal{R}$ . Then the reconstruction probability of the traditional masking is  $Q = P(z|\mathcal{Z})$ , while that of our method is  $P = P(z|\mathcal{Z}, \mathcal{R})$ .

According to the "conditioning reduces entropy" theorem [Cover and Thomas, 2005], knowing another random variable  $Y$  will not increase the uncertainty of  $X$ , i.e.,  $H(X|Y) \leq H(x)$  and the equality holds if and only if  $X$  and  $Y$  are independent. Since in chemical reactions, the reaction centre and reactant are highly correlated, we have  $z$  and  $\mathcal{R}$  are not independent given  $\mathcal{Z}$ . As a result, our method has a lower information entropy for reconstruction than the traditional masking:

$$H(z|\mathcal{Z}, \mathcal{R}) < H(z|\mathcal{Z}), \quad (6)$$

meaning that the choice of masked sub-units becomes more definite under the context of chemical reactions. This allows the model to learn explicit chemical semantics of molecular sub-structures. Moreover, the information gain, i.e., the quantity of reduced uncertainty is given by  $I(z, \mathcal{R}|\mathcal{Z})$ .

## B Detailed Results Analysis on MoleculeACE

### B.1 Detailed Results of SOTA Results on MoleculeACE

We show the detailed performance of 3 best methods including ECFP+SVM,  $REMO_I$ -Graphormer and  $REMO_M$ -Graphormer on 30 sub-tasks of MoleculeACE in Figure 5 and Figure 6, illustrating REMO’s mastery in grasping the Quantitative Structure-Activity Relationship (QSAR).

### B.2 Detailed Results of Ablation Studies on MoleculeACE

The detailed results of the conducted ablation studies on MoleculeACE are depicted in Figure 7 and Figure 8, showcasing the superiority of our contextual pre-training objective over the single molecular-based masking strategy.

## C Case Level Comparison on REMO

To gain deeper insights into the distinctions between  $REMO_M$  and Graphormer-p during the pre-training phase, we perform a detailed analysis of the output logits derived from the mask reconstruction process. The prediction head, responsible for the reconstruction task, generates a vector of length 2401, which corresponds to the 2401 possible 1-hop topological combinations of atoms in the dataset. The primary objective of this prediction head is to accurately classify the masked component using the available dictionary of 2401 tokens. Through this meticulous examination, we obtain additional evidence highlighting the divergent approaches and characteristics of  $REMO_M$  and Graphormer-p throughout the pre-training phase.

As depicted in Figures 9-12, the variations in logits for reconstructing the reaction centre between  $REMO_M$  and Graphormer-p are visualized as square heatmaps of size  $49 \times 49$ , representing the 2401 possible values in the token dictionary. The target label is highlighted by red squares.

## D Evaluation of REMO for Molecular Property Prediction

**Data** Apart from the baselines included in the main text, we evaluate REMO of multiple settings on MoleculeNet [Wu et al., 2018], including physiological properties such as BBBP, Sider, ClinTox, Tox21, and Toxcast, as well as biophysical properties such as Bace, HIV, and MUV. We use the scaffold method to split each dataset into training, validation, and test sets by a ratio of 8:1:1.

**Baselines** We compare our methods with various state-of-the-art self-supervised techniques that are also based on 2D graph, including AttrMask [Hu et al., 2020], GraphMAE [Hou et al., 2022], GraphLoG [Xu et al., 2021], Grover [Rong et al., 2020], Mole-BERT [Xia et al., 2023] and GraphMVP [Liu et al., 2021]. Since USPTO only covers 0.7

Dataset	BBBP	Tox21	MUV	BACE	ToxCast	SIDER	ClinTox	HIV	Avg.
Graphormer-s	67.1(2.0)	73.7(0.4)	58.3(3.2)	70.4(3.9)	65.2(0.5)	63.4(0.5)	72.5(0.3)	71.7(0.5)	67.8
GROVER <sub>base</sub> [Rong et al., 2020]	70.0(0.1)	74.3(0.1)	67.3(1.8)	82.6(0.7)	65.4(0.4)	64.8(0.6)	81.2(3.0)	62.5(0.9)	71.0
GROVER <sub>large</sub> [Rong et al., 2020]	69.5(0.1)	73.5(0.1)	67.3(1.8)	81.0(1.4)	65.3(0.5)	65.4(0.1)	76.2(3.7)	68.2(1.1)	70.8
AttrMask [Hu et al., 2020]	64.3(2.8)	76.7(0.4)	74.7(1.4)	79.3(1.6)	64.2(0.5)	61.0(0.7)	71.8(4.1)	77.2(1.1)	71.2
GraphMAE [Hou et al., 2022]	72.0(0.6)	75.5(0.6)	76.3(2.4)	83.1(0.9)	64.1(0.3)	60.3(1.1)	82.3(1.2)	77.2(0.1)	73.9
GraphLoG [Xu et al., 2021]	72.5(0.8)	75.7(0.5)	76.0(1.1)	83.5(1.2)	63.5(0.7)	61.2(1.1)	76.7(3.3)	77.8(0.8)	73.4
Mole-BERT [Xia et al., 2023]	72.3(0.7)	77.1(0.4)	<b>78.3(1.2)</b>	81.4(1.0)	64.5(0.4)	62.2(0.8)	80.1(3.6)	78.6(0.7)	74.3
GraphMVP [Liu et al., 2021]	68.5(0.2)	74.5(0.4)	75.0(1.4)	76.8(1.1)	62.7(0.1)	62.3(1.6)	79.0(2.5)	74.8(1.4)	71.7
<i>REMO</i> <sub>I</sub> -Graphormer	<b>73.4(1.4)</b>	<b>78.5(0.7)</b>	76.4(0.9)	84.4(0.6)	68.1(0.2)	<b>67.0(1.1)</b>	64.6(6.0)	77.3(1.5)	73.7
<i>REMO</i> <sub>M</sub> -Graphormer	66.8(2.3)	77.4(0.3)	77.5(3.1)	82.0(2.0)	67.5(0.3)	65.8(1.8)	70.1(1.6)	79.6(0.6)	73.3
<i>REMO</i> <sub>IM</sub> -Graphormer	70.1(1.2)	<b>78.5(0.9)</b>	77.4(2.1)	<b>84.5(0.4)</b>	<b>69.2(0.6)</b>	65.4(0.5)	75.2(5.4)	77.4(1.3)	74.7
<i>REMO</i> <sub>IM</sub> -AttrMask	72.4(0.6)	76.4(0.2)	72.1(4.4)	78.3(0.5)	62.8(0.1)	60.5(0.5)	81.3(0.2)	77.0(0.1)	72.6
<i>REMO</i> <sub>IM</sub> -GraphMAE	71.6(0.1)	75.8(0.1)	77.1(2.0)	82.1(0.2)	64.0(0.1)	64.3(0.2)	<b>85.6(1.9)</b>	<b>79.8(0.1)</b>	<b>75.0</b>

Table 6: Comparison between *REMO* and baselines on 8 classification tasks of MoleculeNet.

Dataset	BBBP	Tox21	MUV	BACE	ToxCast	SIDER	ClinTox	HIV	Avg.
AttrMASK	64.3(2.8)	76.7(0.4)	74.7(1.4)	79.3(1.6)	64.2(0.5)	61.0(0.7)	71.8(4.1)	77.2(1.1)	71.2
AttrMASK - USPTO	66.2(1.8)	76.6(0.3)	75.3(0.4)	79.8(0.5)	64.0(0.4)	59.5(0.5)	66.1(2.7)	78.2(1.2)	70.71
<i>REMO</i> <sub>IM</sub> -AttrMASK	72.4(0.6)	76.4(0.2)	72.1(4.4)	78.3(0.5)	62.8(0.1)	60.5(0.5)	81.3(0.2)	77.0(0.1)	72.6
GraphMAE	72.0(0.6)	75.5(0.6)	76.3(2.4)	83.1(0.9)	64.1(0.3)	60.3(1.1)	82.3(1.2)	77.2(0.1)	73.9
GraphMAE - USPTO	72.8(1.1)	75.6(0.5)	71.8(1.1)	83.0(0.6)	63.8(0.3)	58.9(0.5)	79.5(0.5)	78.3(0.8)	72.97
<i>REMO</i> <sub>IM</sub> -GraphMAE	71.6(0.1)	75.8(0.1)	77.1(2.0)	82.1(0.2)	64.0(0.1)	64.3(0.2)	85.6(1.9)	79.8(0.1)	75.0

Table 7: Results for Ablation Study of *REMO*<sub>IM</sub>-AttrMASK and *REMO*<sub>IM</sub>-GraphMAE on MoleculeNet.

million molecules, we propose to continuously pre-train AttrMask and GraphMAE with both masked reaction centre reconstruction and identification objectives, denoted as *REMO*<sub>IM</sub>-AttrMask and *REMO*<sub>IM</sub>-GraphMAE, respectively.

**Finetuning** We append a 2-layer MLP after the pre-trained model to get the logits of property predictions and minimize binary cross-entropy loss for the classification tasks during fine-tuning. ROC-AUC(%) is employed as evaluation metric for these classification tasks. All methods are run 3 times with different seeds and the mean and deviation values are reported.

**Results** Table 6 shows that: (1) both pre-training objectives in *REMO* significantly improve the prediction performances, i.e. increasing from 67.8% (supervised Graphormer denoted as Graphormer-s) to 73.3% (*REMO*<sub>M</sub>-Graphormer) and 73.7% (*REMO*<sub>I</sub>-Graphormer), respectively. (2) By using only 0.7 million molecules for pre-training, *REMO* outperforms other methods such as MoleBERT and Grover which uses much larger data (i.e. 2 and 10 million molecules respectively), demonstrating the effectiveness of our contextual pre-training strategy. (3) *REMO*'s performance can be further improved when combined with other methods. As compared to the original AttrMask and GraphMAE, *REMO* improves their results from 71.2%/73.9% to 72.6%/75.0%, respectively.

## E Ablation Study of *REMO*-AttrMASK and *REMO*-GraphMAE

In Table 7 *REMO*<sub>IM</sub>-AttrMASK and *REMO*<sub>IM</sub>-GraphMAE undergo continuous pretraining using the updated objective function. We acknowledge that distinguishing between the performance improvement stemming from increased pretraining data and the impact of the modified objective function can be unclear. To address this concern, we have conducted comprehensive ablation studies specifically focused on *REMO*<sub>IM</sub>-AttrMASK and *REMO*<sub>IM</sub>-GraphMAE. The aim of these studies is to elucidate the precise influence of the objective function alteration.

AttrMask - USPTO and GraphMAE - USPTO involve consistent pretraining of the original model using molecules from the USPTO dataset. Although they exhibit comparable performance to the original models across numerous benchmarks, they do not achieve comparable results to *REMO* for certain tasks. Remarkably, when introducing USPTO data through the original method, the overall average score even experiences a slight reduction. Nonetheless, the advantage stemming from the new objective function remains conspicuous.

## F Imbalanced Distribution in Masked Reaction Centre Reconstruction

The potential challenge of imbalanced distribution in Masked Reaction Centre Reconstruction has been thoroughly examined. Specifically, we assessed the distribution of atoms and their adjacent bonds in both the ZINC dataset and the USPTO dataset, adhering to the reconstruction target construction approach outlined in Rong et al. [2020]. To ensure clarity, we created a dictionary that encompasses atoms along with their neighboring bonds. This facilitated an in-depth analysis of the distribution of reconstruction targets. We conducted this analysis across three significant datasets: ZINC, the broader USPTO dataset, and the reaction centres within USPTO.

Upon analyzing the distribution of atom and edge types, we selected the top 20 labels with the highest frequencies for closer examination, addressing the issue of label imbalance.

### F.1 ZINC Dataset Atom Distribution

As shown in Figure 13, in the ZINC dataset, the top 20 atom labels constituted approximately 76.54% of the dataset, with the highest frequency label being *carbon connected with two aromatic bonds* at a rate of 22.58%.

### F.2 USPTO Dataset Atom Distribution

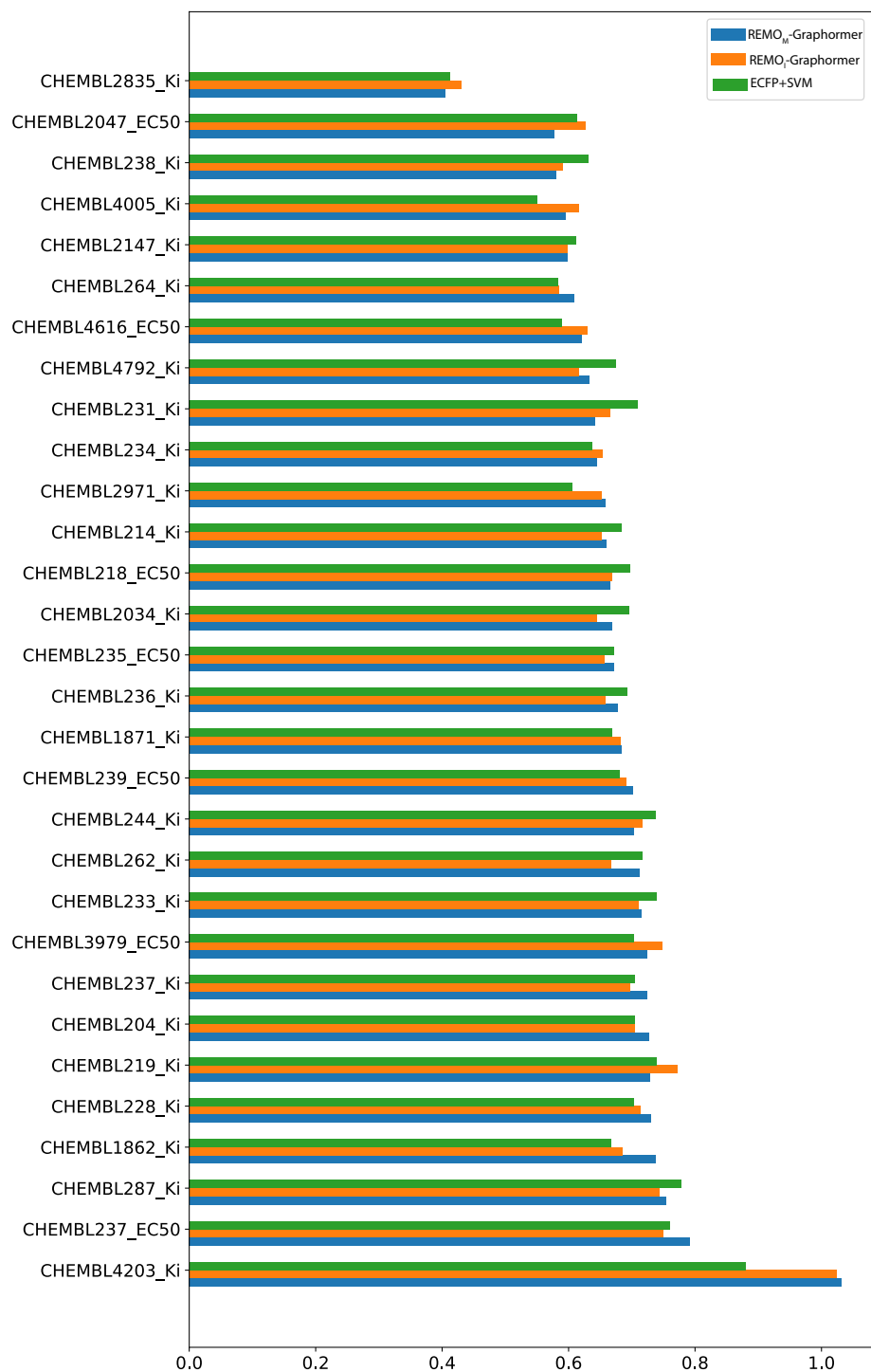
As shown in Figure 14, within the USPTO dataset, the top 20 atom labels accounted for around 71.53% of the dataset, and the most frequent label was *carbon connected with two aromatic bonds* at a rate of 19.79%.

### F.3 Reconstruction Target Atom Distribution

As shown in Figure 15, in the reconstruction targets of USPTO, the top 20 atom labels represented approximately 63.58% of the total reconstruction targets, with the label *nitrogen connected with a single bond* occurring most frequently at a rate of 8.62%.

It is noteworthy that the issue of imbalanced distribution exists in both the ZINC and USPTO datasets, with a prevalence of carbon atoms. However, within the context of masked reaction centre reconstruction, this concern is mitigated compared to the random masking of atoms.

Indeed, the distribution of atom types within the reconstruction target is an advantageous aspect of REMO compared to other baseline models. The reconstruction target's relative balance is a notable strength when compared to the data treatment employed by other baselines.

Figure 5: RMSE of  $REMO_M$ -Graphormer,  $REMO_I$ -Graphormer and ECFP+SVM on MoleculeACE

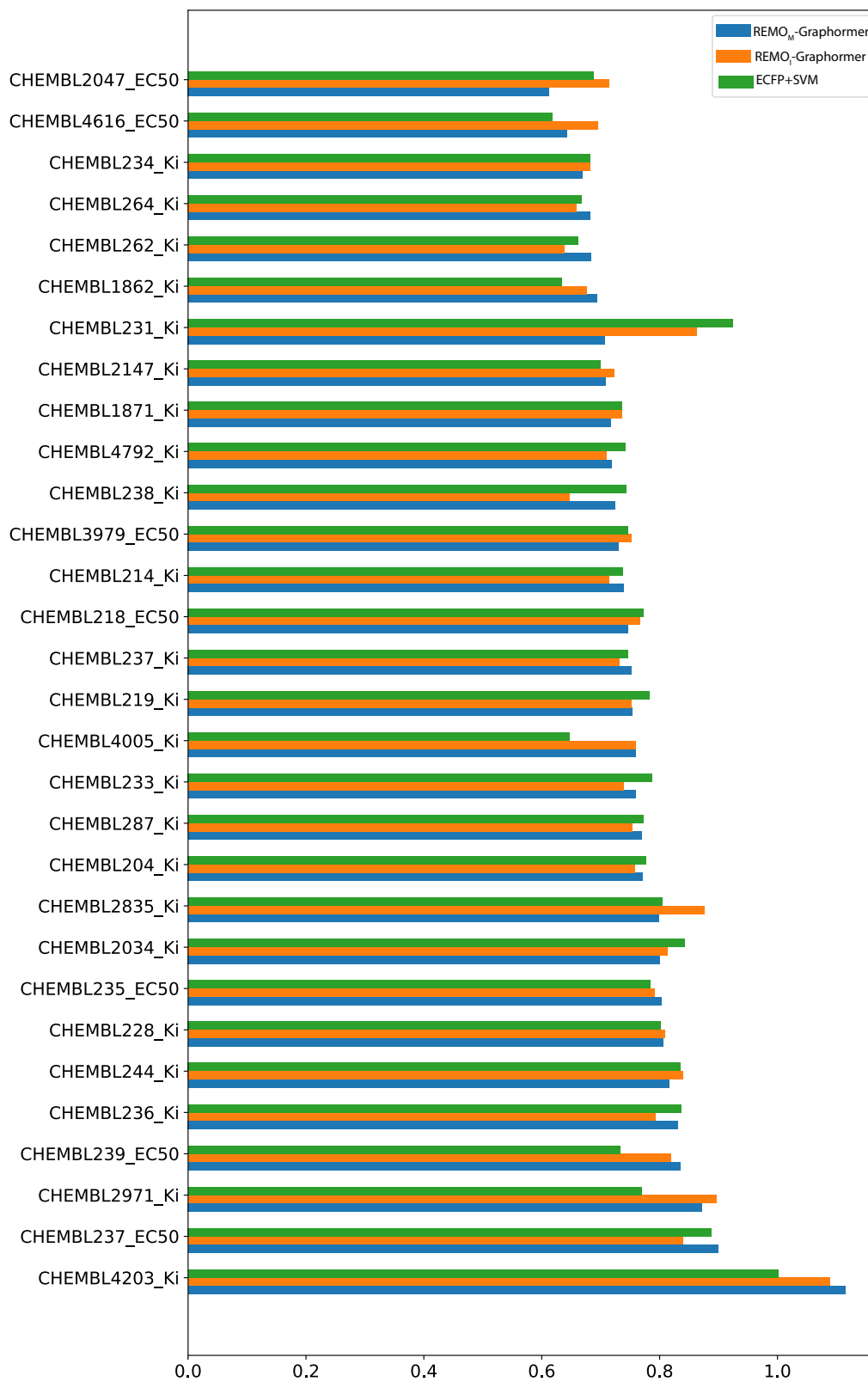


Figure 6: RMSE<sub>diff</sub> of  $REMO_M$ -Graphormer,  $REMO_I$ -Graphormer and ECFP+SVM on MoleculeACE

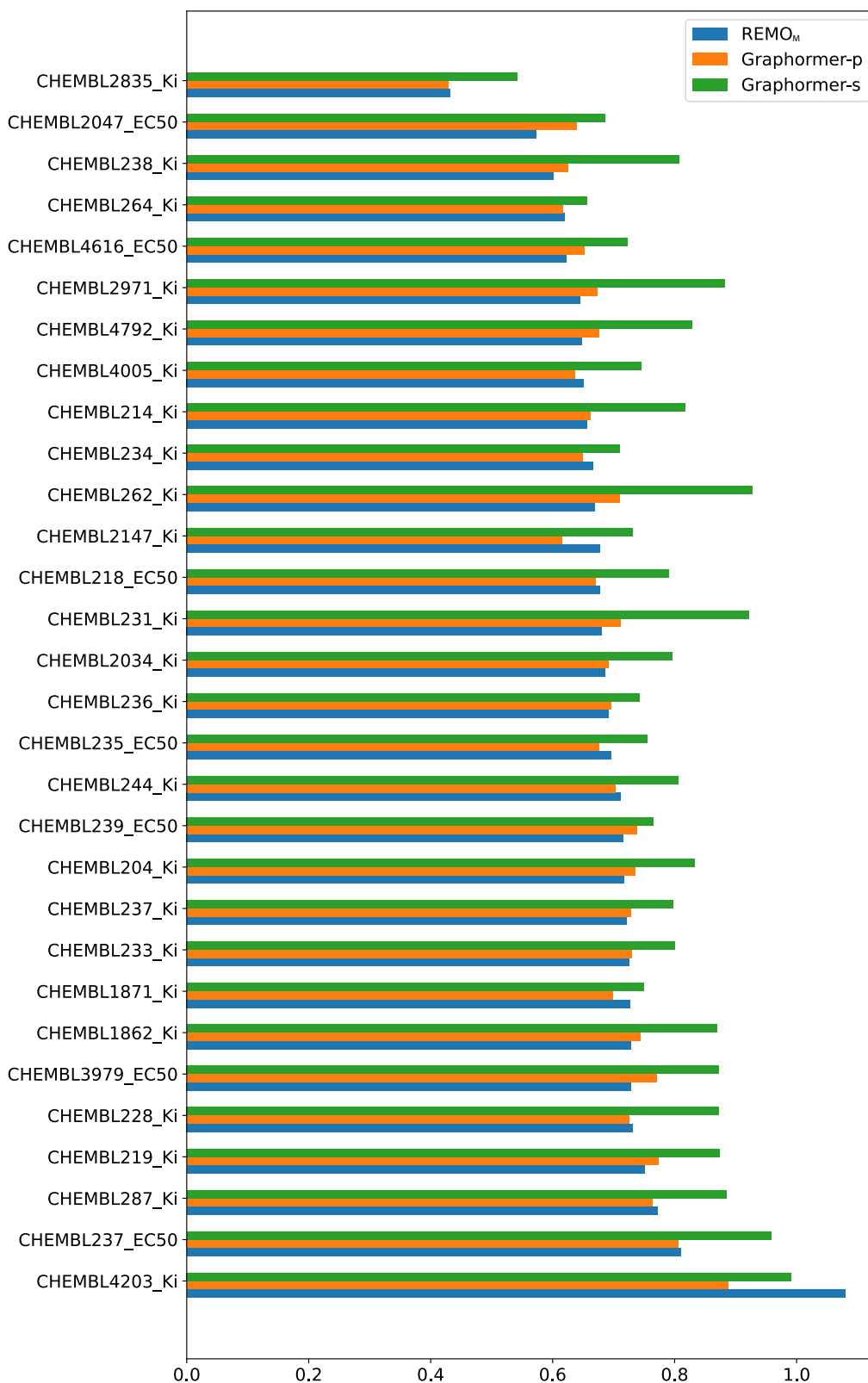


Figure 7: RMSE of  $REMO_M$ , Graphormer-p, and Graphormer-s on MoleculeACE

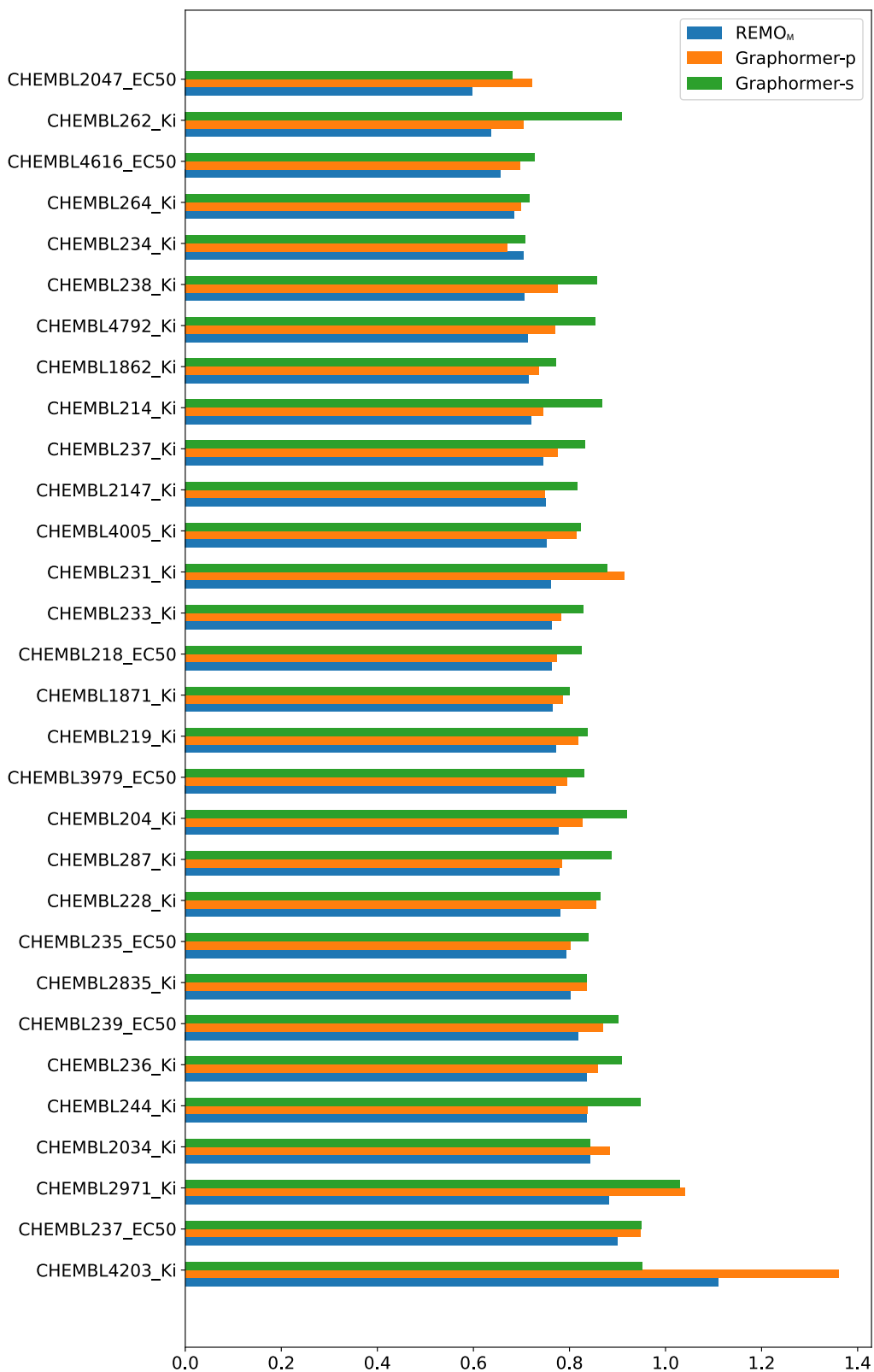


Figure 8:  $RMSE_{diff}$  of  $REMO_M$ , Graphormer-p, and Graphormer-s on MoleculeACE

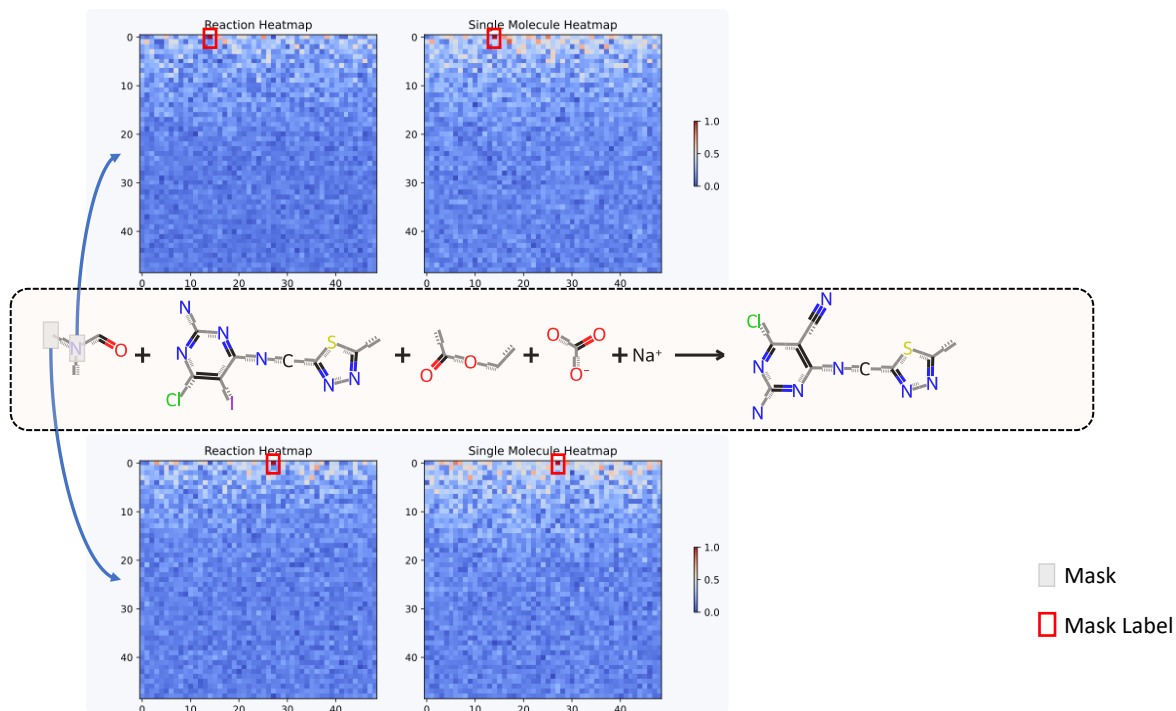


Figure 9: Case 1: Reconstruction of the reaction centre involving a carbon atom and a nitrogen atom.  $REMO_M$  exhibits higher confidence in the reconstruction choice, while Graphormer-p shows increased uncertainty (evidenced by higher predicted logits for the masked nitrogen atom in indices 17 to 30, and for the masked carbon atom in indices 3 to 10).

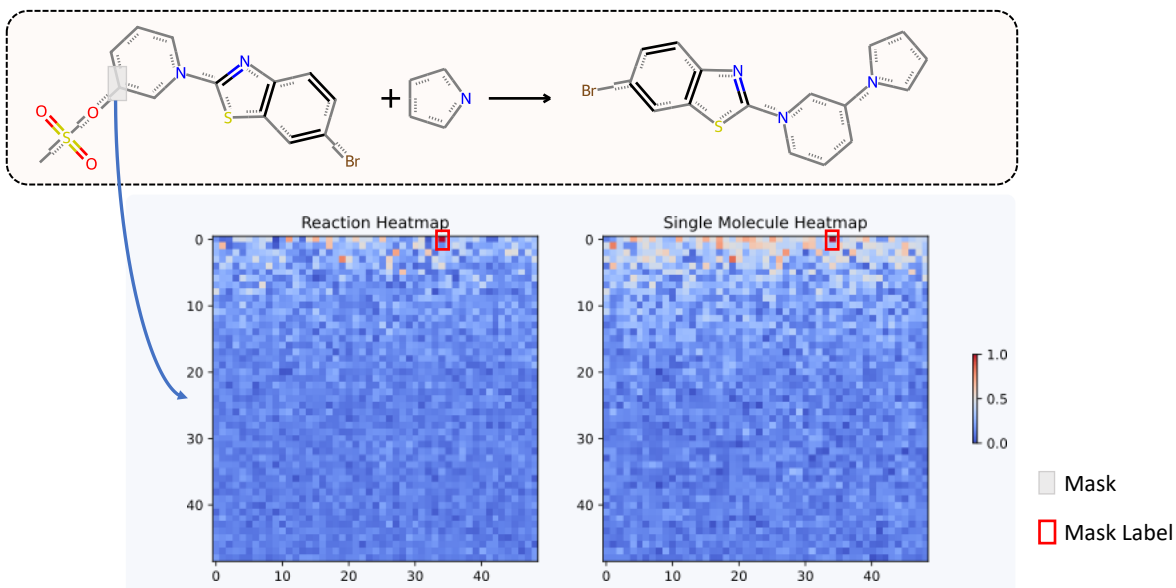


Figure 10: Case 2: Reconstruction of the reaction centre involving a carbon atom in a substituent reaction. In the absence of reaction context, Graphormer-p exhibits higher confusion, as indicated by the flatter distribution of logits observed in the heatmap.

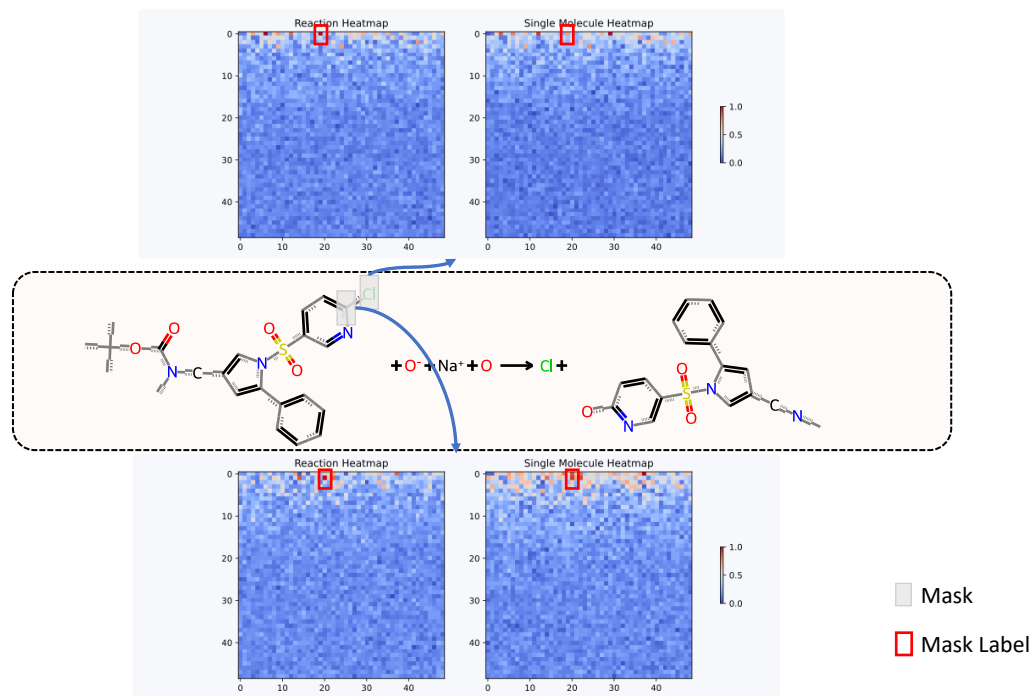


Figure 11: Case 3: Reconstruction of the reaction centre involving a carbon atom and a chlorine atom. Graphormer-p fails to reconstruct the chlorine atom in the absence of reaction context, whereas  $REMO_M$  accurately identifies the correct answer. Additionally,  $REMO_M$  demonstrates a more definitive choice for mask reconstruction of the carbon atom.

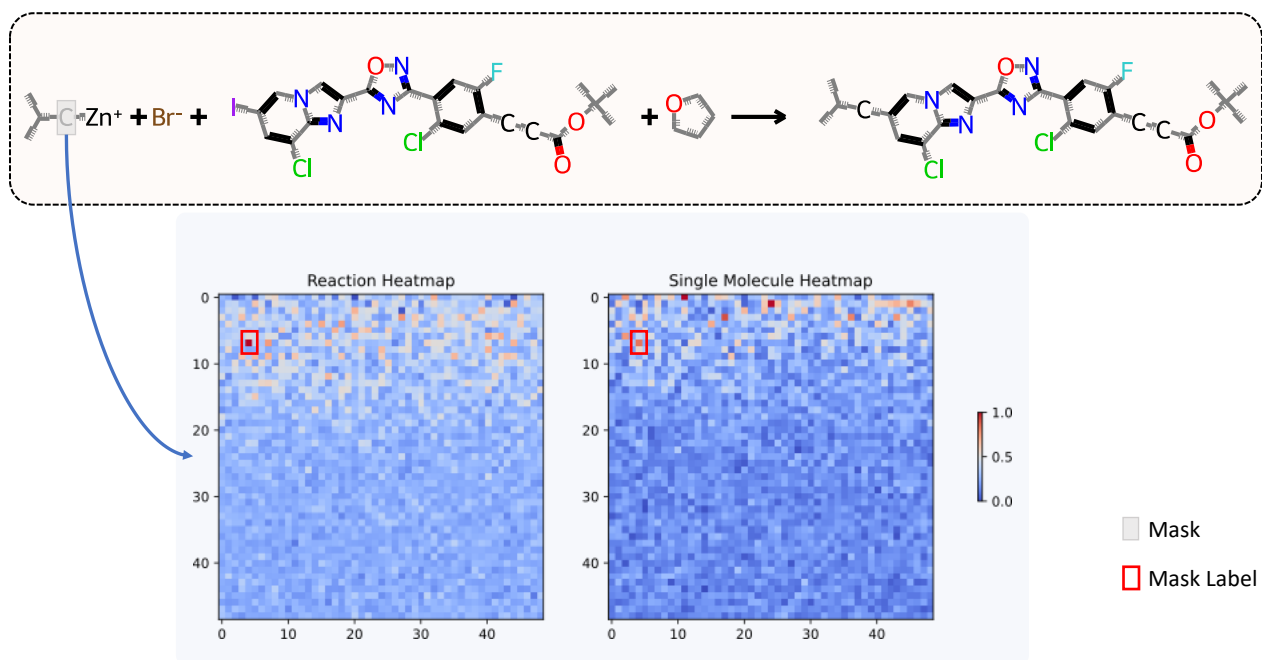


Figure 12: Case 4: The reaction involves the substitution of an iodine atom by an organozinc compound. In the absence of reaction context, Graphormer-p fails to reconstruct the reaction centre, specifically a carbon atom, whereas  $REMO_M$  successfully identifies the correct reaction centre.

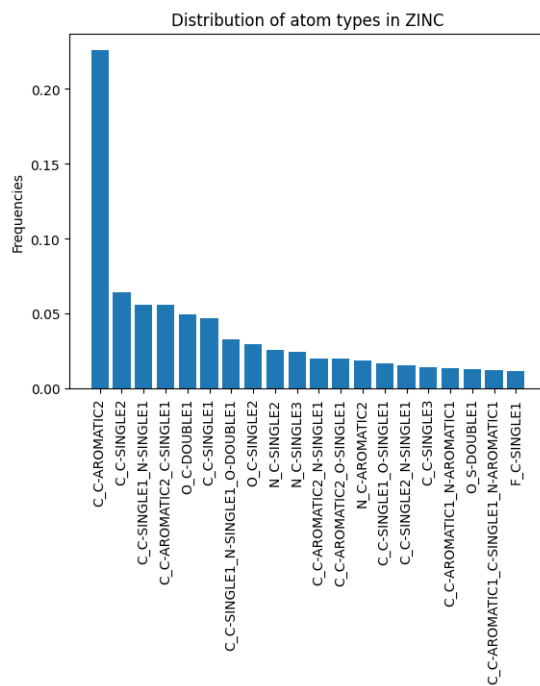


Figure 13: Distribution of Atom Types in ZINC

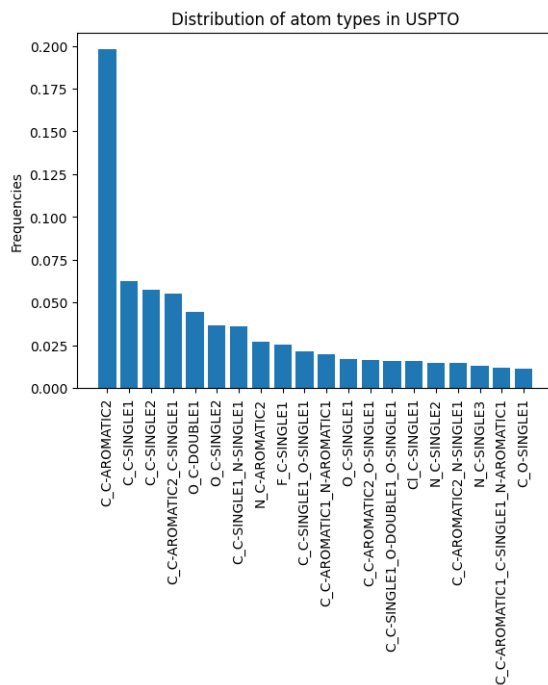


Figure 14: Distribution of Atom Types in USPTO

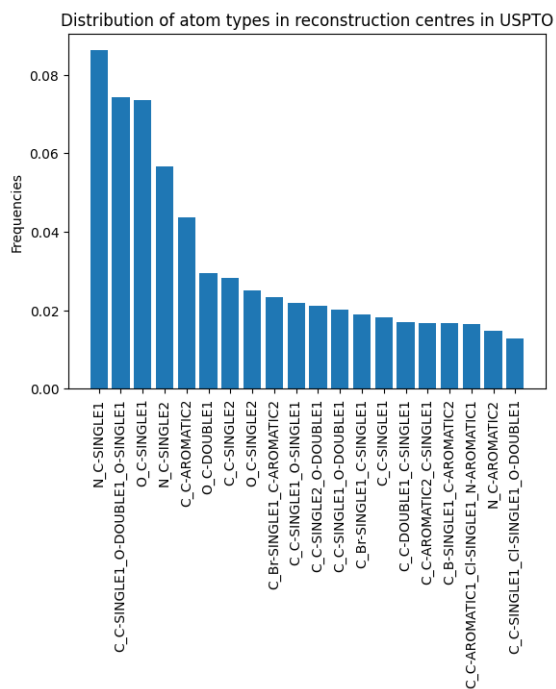


Figure 15: Distribution of Atom Types in reconstruction centres in USPTO